

12.5 CURRENT AND FUTURE PLANS FOR THE AP CLUTTER MITIGATION SCHEME

Cathy Kessinger, Scott Ellis, Joseph Van Andel, Jaimi Yee and John Hubbert
National Center for Atmospheric Research
P.O. Box 3000
Boulder, CO 80305

1. Introduction

Implementation of the AP Clutter Mitigation Scheme is underway within the WSR-88D system as part of the Open Radar Product Generator (ORPG; Saffle et al. 2001). Once fully implemented, this scheme will improve the radar base data quality by identification and removal of ground clutter produced under anomalous propagation (AP) conditions. The current WSR-88D quality control system removes ground clutter that is present during normal propagation conditions by application of clutter bypass maps. AP ground clutter requires manual application of additional clutter filters. The AP Clutter Mitigation Scheme is working toward full automation of ground clutter filter specification and control. The first step in this implementation was achieved when the AP Clutter Detection Algorithm (APDA) was deployed during Build 2 of the ORPG in September 2002. Output from the APDA is available for perusal on the ORPG Clutter Filter Control panel and is expressed in terms of “clutter likelihood values” between 0-100, with 100 meaning that clutter is very likely present.

The AP Clutter Mitigation Scheme (Ellis et al. 2003; Kessinger et al. 2002) consists of three parts: 1) the Radar Echo Classifier (REC) of which the APDA is one module and the Precipitation Detection Algorithm (PDA) is a second module, 2) the Reflectivity Compensation Scheme (Z-Comp), and 3) clutter filter specification and control. The Enhanced Preprocessing Subsystem (EPRE; O’Bannon and Ding, 2003) is an enhanced version of the Precipitation Pre-processing Subsystem (PPS; Fulton et al. 1998; O’Bannon 1998) and is used to compute radar-derived rainfall estimates. The initial version of EPRE is planned for implementation in ORPG

Build 5 in spring 2004 and will use the APDA to remove clutter from the hybrid scan. Once fully deployed within ORPG, output from the REC APDA, the REC PDA and the Z-Comp will be input into the EPRE.

The Sigmat Corporation RVP8 digital signal processor will be installed on the WSR-88D systems as part of the Open Radar Data Acquisition (ORDA; Elvander et al. 2001). The RVP8 has also been installed on the NCAR S-band dual-Polarization radar (S-Pol) (Keeler et al. 2000) as a parallel processor (Keeler et al. 2003). The RVP8 processor will allow the use of spectral domain processing and will facilitate greater improvement in base data quality. Modification of the AP Clutter Mitigation Scheme to accommodate the new ORDA processor is planned and some preliminary results are presented.

This paper discusses the REC and the Z-Comp algorithm performance when data are input from the Denver WSR-88D (KTFG) during a snow storm on 18-19 March 2003. New, spectral domain variables for the REC are presented.

2. Radar Echo Classifier

The radar echo classifier (REC) is an expert system that uses “fuzzy-logic”, data fusion techniques (Kosko, 1992) to estimate the type of scatterer measured by a radar and uses the moment fields of reflectivity, radial velocity and spectrum width as input. The REC is described in detail in Kessinger, et al. (2003). Currently, three algorithms have been designed and tested: the AP detection algorithm (APDA) detects regions of AP ground clutter return, the precipitation detection algorithm (PDA) defines convective and stratiform precipitation regions in combination, and the sea clutter detection algorithm (SCDA) defines regions of clutter caused by the radar beam interacting with the sea surface.

Corresponding author address: Cathy Kessinger, NCAR, P.O. Box 3000, Boulder, CO 80307; email: kessinge@ucar.edu

The APDA and the PDA were developed using data from several WSR-88Ds and the S-Pol (Kessinger et al. 1999). The SCDA was developed, tested and deployed on the United Arab Emirates (UAE) Doppler radars. Real-time deployment of the REC has been accomplished on the S-Pol at various field experiments since June 2000.

3. Reflectivity Compensation Scheme

The Reflectivity Compensation scheme (Z-Comp) uses a Gaussian approximation for the precipitation spectra and a simulated WSR-88D clutter filter to estimate the correction to offset the clutter-filter-induced (negative) bias in the reflectivity. Details of the algorithm design and implementation are in Ellis (2001). The Z-Comp method has been tested quantitatively using WSR-88D time-series data (aka Archive 1) collected at the Memphis (KNQA) WSR-88D and has been run operationally on the S-Pol since 2001.

Within the AP Clutter Mitigation Scheme, output from the REC APDA and the PDA determine where the Z-Comp scheme is applied such that only regions of precipitation are compensated. This prevents undesired compensation of reflectivity values within ground clutter return.

4. Radar Systems

The WSR-88Ds are 10 cm wavelength radars with single polarization. The S-Pol is a 10 cm wavelength, dual polarization radar. The S-Pol uses a four-pole elliptical, high pass ground clutter filter with passband edges of $\pm 0.5 \text{ m s}^{-1}$. The WSR-88D clutter filter for low suppression has passband edges of $\pm 1.2 \text{ m s}^{-1}$ and for medium suppression has passband edges of $\pm 1.6 \text{ m s}^{-1}$. Because of its comparatively narrow width, the S-Pol ground clutter filter removes less data from the power spectra when compared to a WSR-88D.

5. Current Status of the AP Clutter Mitigation Scheme

The Enhanced Preprocessing Subsystem (EPRE; O'Bannon and Ding, 2003) will be implemented within ORPG Build 5 in spring 2004. The EPRE is an updated version of the PPS and will use the APDA to remove clutter contamination during construction of the hybrid scan. The PDA and the Z-Comp algorithms are planned to be implemented in the ORPG Build 6 or 7. Once implemented, the

PDA and the Z-Comp output will be input into EPRE to further enhance precipitation estimates by correcting for the clutter filter bias in the reflectivity.

The last REC algorithm to be developed and eventually deployed within the ORPG will be the stratiform/convective partition algorithm based on the Steiner et al. (1995) technique. This algorithm will be similar to the PDA except that each type of precipitation will be treated separately. Once ORPG development is completed for the AP Mitigation Scheme, efforts will be directed at modifying the scheme for the ORDA environment.

6. Results from Denver KFTG

To illustrate the Z-Comp algorithm, a snow case was selected using the Denver WSR-88D (KFTG) located to the east of Denver and approximately 60 km east of the Rocky Mountains. This case was selected from 18-19 March 2003 because of the stratiform nature of the reflectivity return and because of the storm's long duration and steady prevailing wind direction during the period of interest. The negative bias induced by application of the ground clutter filters is more apparent in stratiform precipitation compared to convective precipitation. Attempts to compare the rainfall accumulations of the filtered and compensated reflectivity fields in convective situations have been stymied by the rapid movement of the storms and their uncanny ability to avoid surface stations. The steady prevailing wind direction in this snow case allows a large, negative bias to persist in particular locations, useful when comparing the radar-derived, water equivalent snowfall amounts to surface measurements.

As part of the Federal Aviation Administration (FAA) Winter Storms Product Development Team, several snow gauges have been deployed in the Denver Metropolitan region. Data from these snow gauges will be compared to the KFTG radar-derived snowfall accumulation using the filtered and compensated reflectivity fields to examine the ZComp performance. Data from two ASOS stations are also examined. Data are not yet available from the NCAR Marshall Field site (indicated by "Mar" in Figures 4 and 5) but is expected by the time of the conference.

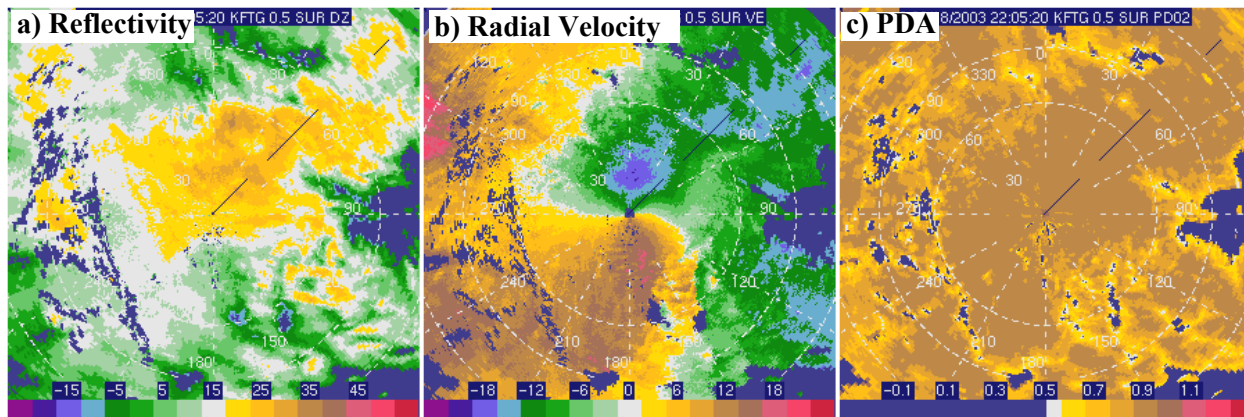


Figure 1. Data are shown from the Denver WSR-88D (KFTG) on 18 March 2003 at 2205 UTC. Fields shown are the a) filtered reflectivity (dBZ), b) the radial velocity ($m s^{-1}$), and c) output from the REC Precipitation Detection Algorithm (PDA) thresholded at 0.5 interest values. The 0.5 degree elevation angle is shown with range rings at 30 km intervals.

Also, this is the first time that the Z-Comp algorithm has been applied to winter precipitation conditions and shows that the technique is applicable to warm and cold season precipitation.

Figure 1 shows the reflectivity, radial velocity and the REC PDA output fields from 18 March 2003 at 2205 UTC. At this time, the most intense reflectivity is located over and north of KFTG. The winds are from the north and remain very steady during the eleven hour period that is analyzed from 18 UTC on the 18th to 5 UTC on the 19th of March. The PDA performs well at detecting the snow regions as seen in Figure 1c. The APDA (not shown) performs well by not identifying

precipitation as clutter.

To show the negative bias in the reflectivity field, a higher magnification of the reflectivity field is shown in Figure 2a. Figure 2b shows the reflectivity field after application of the Z-Comp algorithm to correct the reflectivity bias while Figure 2c shows the difference between the compensated and filtered reflectivity fields. Notice that the reflectivity difference is about 4 dB at maximum.

Using the snow accumulation algorithm described by Super and Holyrod (1997), and after applying the dielectric factor (Smith, 1984), the water equivalent snowfall rate (S) is calculated from

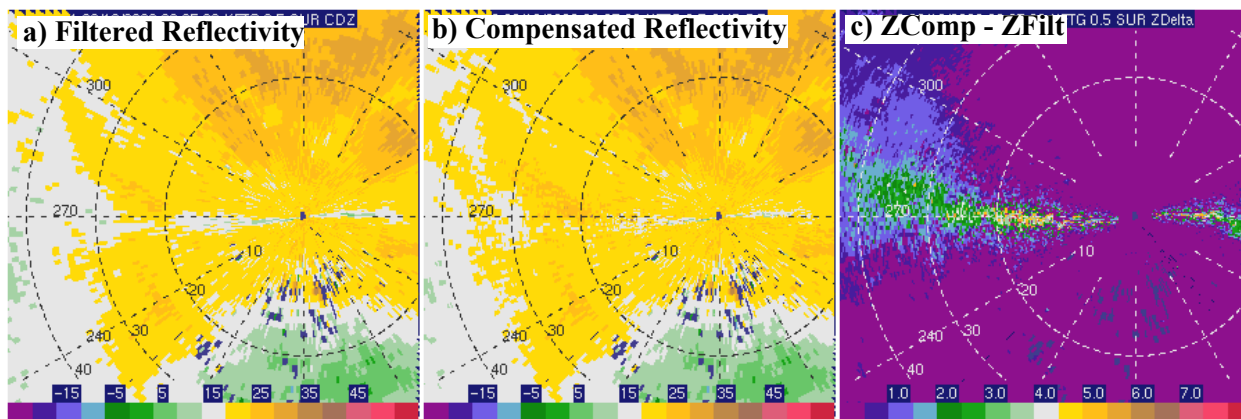


Figure 2. For the same data shown in Figure 1, results from the ZComp algorithm are shown. Fields shown are the a) filtered reflectivity (dBZ), b) the compensated reflectivity (dBZ) and c) the difference of ZComp minus ZFilt (dBZ). Range rings are at 10 km intervals.

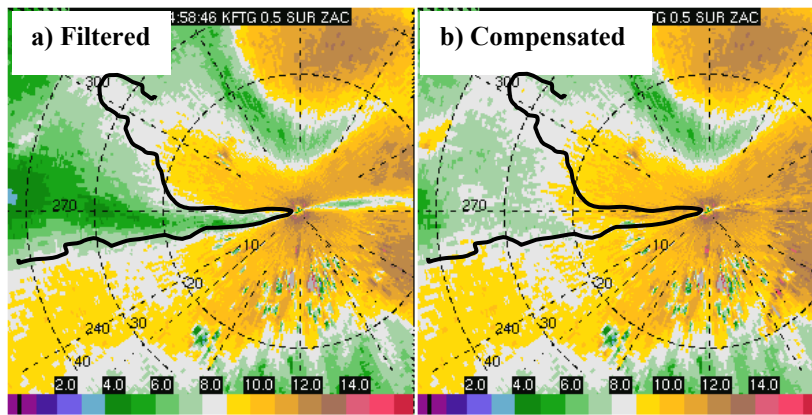


Figure 3. Snow accumulation (mm) is derived from Denver WSR-88D (KFTG) data on 18-19 March 2003 from 18 UTC on the 18th to 5 UTC on the 19th. Fields shown are a) snow accumulation using the filtered reflectivity and b) the snow accumulation using the compensated reflectivity. The bold line shows the 7.5 mm contour from the filtered reflectivity results.

$$S = 0.089165Z_e^{0.5} \quad \text{Eqn 1}$$

where S is expressed as mm hr^{-1} , and Z_e is expressed as $\text{mm}^6 \text{m}^{-3}$. Integration of S over a specified time period gives the snowfall (water equivalent) accumulation. For this case, the snowfall accumulation is calculated over the eleven hour period mentioned above. Snow accumulation is shown with the filtered reflectivity data as input (Figure 3a) and with the compensated reflectivity as input (Figure 3b). Notice how the Z-Comp correction allows a more continuous region of snow accumulation to be derived without the negative bias induced by the clutter filter. The maximum difference in water equivalent snow accumulation is about 4 mm within 30 km of KFTG within small regions to the east and west of the radar location (where the radial velocity was near zero), with maximum differences of about 2 mm in regions farther to the west-northwest. Near the radar, the approximate change in snowfall accumulation is from about 6 mm to 10 mm, a significant difference.

To compare the surface measurements of water-equivalent snowfall accumulation, four surface stations are used. Their locations are indicated in Figures 4 and 5. Unfortunately, a data outage exists in two of the stations, with data ceasing after 2215 UTC. For that reason, storm total accumulation results are shown for two time periods: 1800-2215 UTC (Figure 4) and 1800-0500 UTC (Figure 5).

In Figure 4, the two stations NW of KFTG within 20 km range are located near Denver International Airport (DIA). For this time interval, these stations

are reporting 4 and 6 mm of water equivalent snowfall amounts. Unfortunately, these two stations are located to the north of the maximum bias induced by the clutter filter. This is apparent in the radar-derived accumulation because the values in a) and b) are identical. The radar-derived accumulation is about 5 mm and compares well to the surface measurement. However, the surface station to the SW of KFTG measured only a trace of accumulation during this period compared to the radar-derived amount of 4 mm. At this point in this investigation, the reason for the larger discrepancy between the two is not known. However, it is interesting to note that this surface station is about 40 km from the radar. Perhaps the radar beam is not adequately measuring snowfall very close to the surface.

For the longer time interval, only one surface station is currently available for comparison (Figure 5). This station is one of the DIA stations. The surface station measured 11 mm of water equivalent, snowfall accumulation and compares well to the ZComp results from the filtered and compensated reflectivity fields. Both radar-derived accumulations are about 10 mm.

Data from the Marshall Field site are eagerly anticipated because this site is within the region of compensated reflectivity (Figure 2c).

7. Future Plans for the AP Clutter Mitigation Scheme

For ORDA, the AP Clutter Mitigation Scheme will be adapted to incorporate spectral domain processing techniques. The Sigmet Corporation's

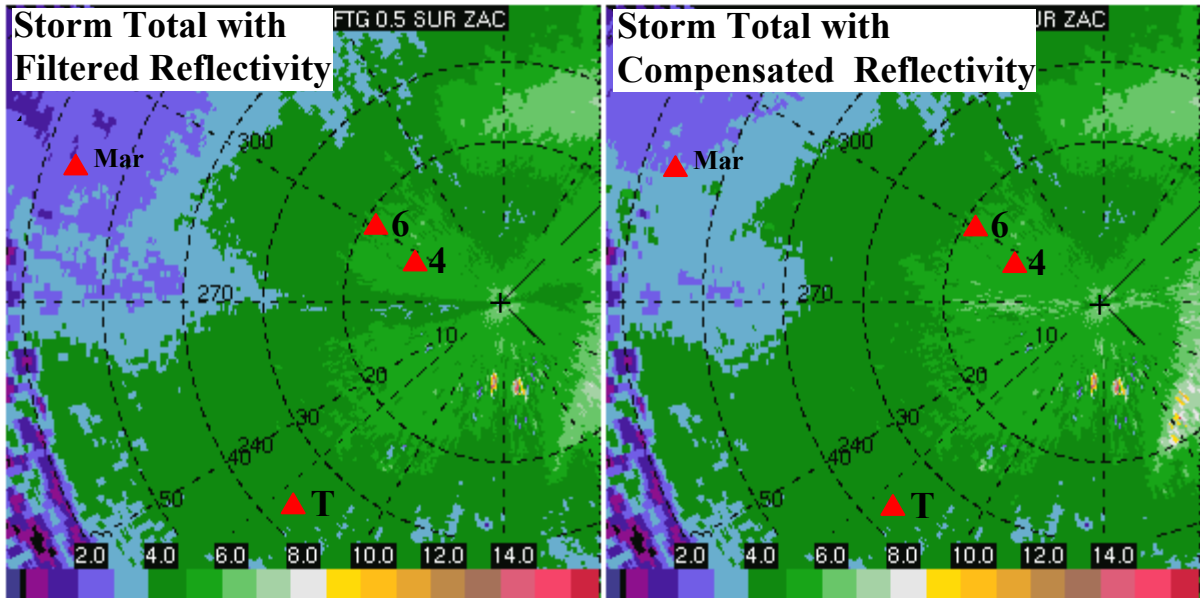


Figure 4. Snowfall, water-equivalent, accumulation (mm) using KFTG data from 18 March 2003 over the time period of 1800-2215 UTC. Fields shown are the a) storm total accumulation using the filtered reflectivity and b) storm total accumulation using the compensated reflectivity. Red triangles indicate position of surface stations with snowfall measurement devices. Measured water equivalent accumulation (mm) is noted to the right of each triangle, with “T” indicating a trace amount of accumulation. Surface data from the Marshall Field site (“Mar”) are not yet available.

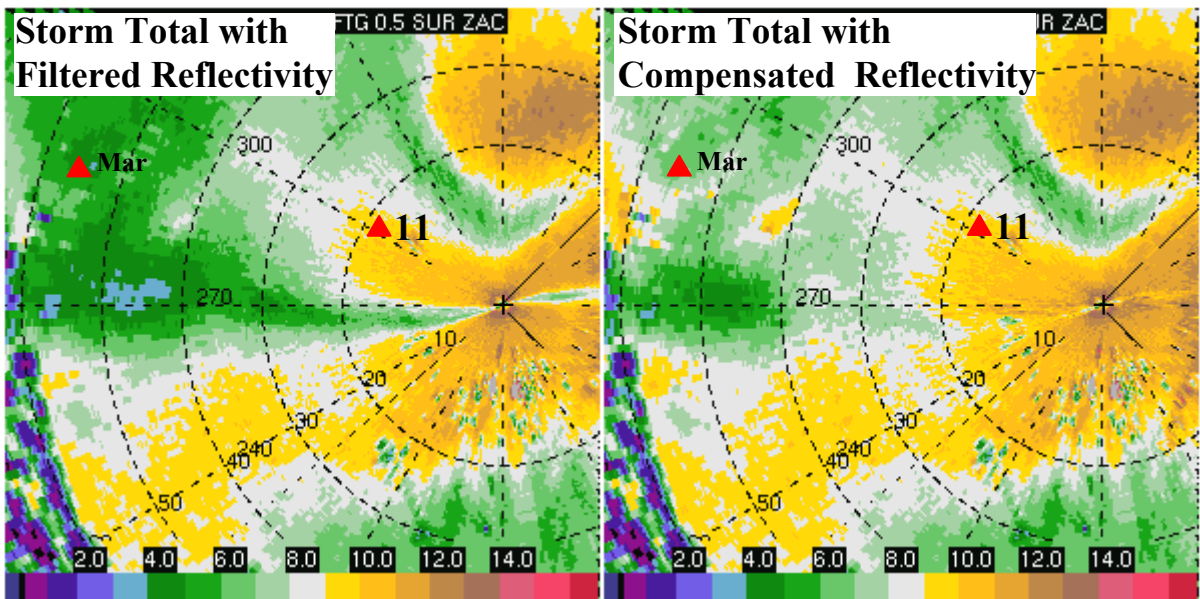


Figure 5. Same as Figure 4 except for a longer time interval on 18-19 March 2003 from 1800-0500 UTC.

RVP8 digital signal processor will be the new processor for the WSR-88D and is planned for deployment on Build 6. The RVP8 has also been

installed on the NCAR S-Pol (Keeler et al, 2003). The RVP8 allows various spectral processing techniques to be used for clutter filter removal that

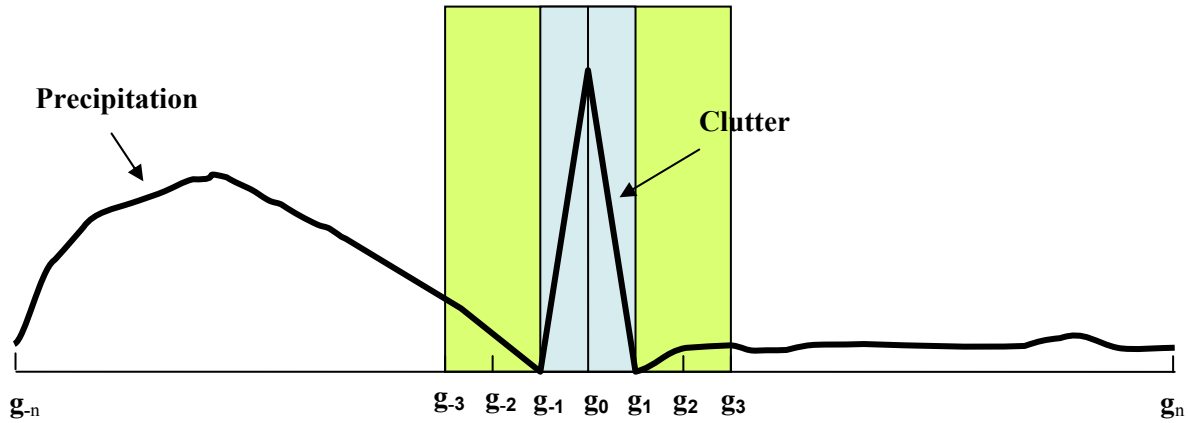


Figure 6. An idealized power spectrum that contains precipitation and clutter return. The velocity index is indicated by “ g_i ” with indices ranging from $-n$ to $+n$, the limits of the Nyquist velocity. The blue region encloses the “clutter power” which corresponds to the power in the velocity indices of g_{-1} , g_0 and g_1 , and is termed “ C_p ”. The green regions contain the “power near zero” at the velocity indices of g_{-3} , g_{-2} , g_2 and g_3 and are termed “ P_{nz} ”.

should lead to additional enhancements in radar data quality. Having RPV8 on both the S-Pol and the WSR-88D will expedite technique development and deployment.

The ability to create new feature fields for input into the REC will be augmented with spectral domain processing. Two new variables have been designed and are presented here. While they have not yet been incorporated as part of the REC APDA or PDA, they will be tested by conference time for a few, selected cases.

Figure 6 shows an idealized power spectrum, $F(g_i)$, where g_i is the velocity index with g_n corresponding to the Nyquist velocity and where $F(g_i)$ is the power at the g_i velocity index. In this simple example, it is assumed that the duration of the time series samples yields a velocity increment (Δg) of about 0.5 m s^{-1} such that the majority of the clutter power is contained in the spectral points g_0 , g_{-1} and g_1 . The large broad “bump” to the left of the clutter is precipitation return. Comparison of the power values at various points in the spectra will yield useful information and help to discriminate clutter from precipitation.

For example, calculating the “clutter power” (C_p) can be done as follows:

$$C_p = \sum [F(g_0) + F(g_{-1}) + F(g_1)] \quad \text{Eqn 2}$$

where $F(g_i)$ corresponds to the power at the i^{th} velocity index. The C_p contains the power that is indicated by the blue region in Figure 6. Calculating the “power near zero” (P_{nz}) is done as follows:

$$P_{nz} = \sum [F(g_{-3}) + F(g_{-2}) + F(g_2) + F(g_3)]. \quad \text{Eqn 3}$$

The P_{nz} contains the power to either side of the C_p region and is indicated by the green regions in Figure 6. The “total power” (“ P_{tot} ”) is the summation of the power at all velocity indices and is calculated as follows:

$$P_{\text{tot}} = \sum_{-n}^n F(g_i) \quad \text{Eqn 4}$$

where i is summed from $-n$ to $+n$.

Using these equations, two new variables are defined and are termed “Ratio 1” and “Ratio 2”. They are calculated as follows:

$$\text{Ratio 1} = C_p / (P_{\text{tot}} - C_p) \quad \text{Eqn 5}$$

and

$$\text{Ratio 2} = C_p / P_{nz}. \quad \text{Eqn 6}$$

These variables should prove useful in

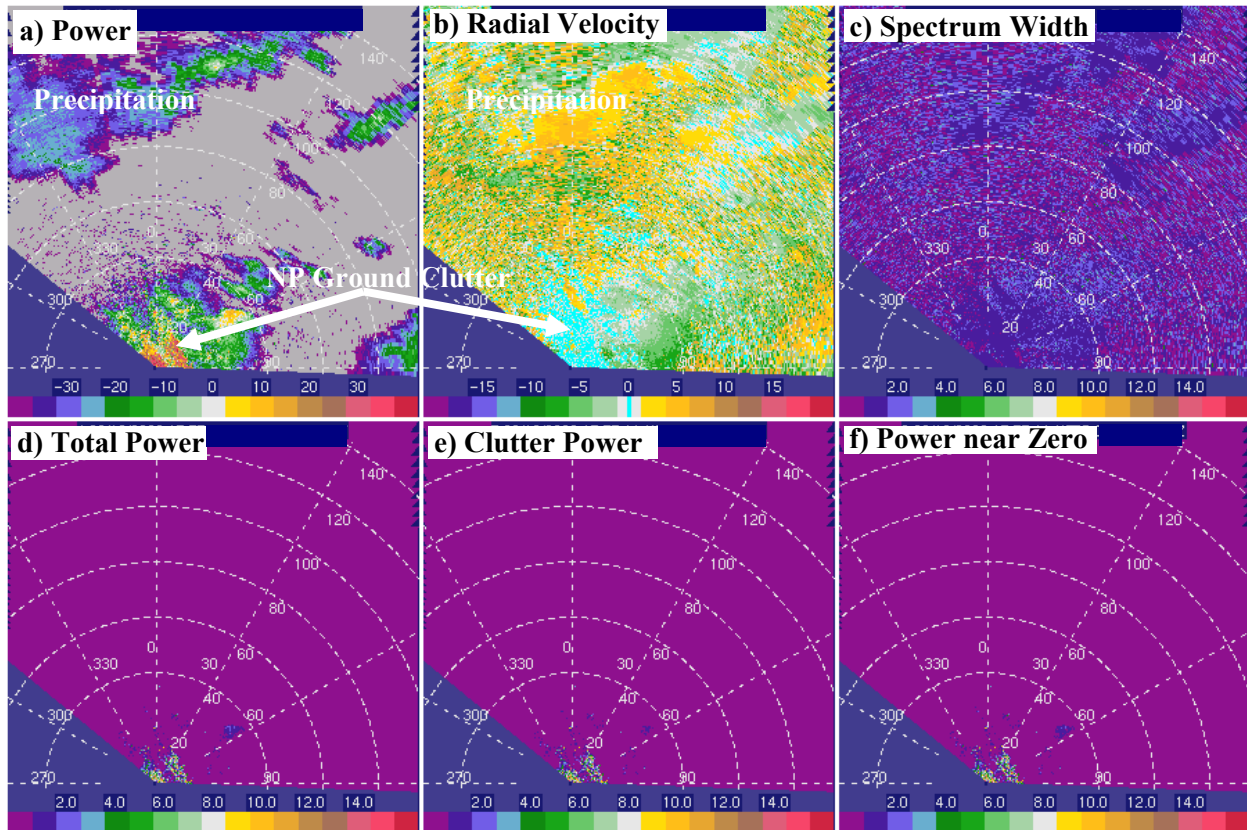


Figure 7. An example of spectral domain variables as calculated from KOUN time series data. Fields shown are a) reflectivity (dBZ), b) radial velocity ($m s^{-1}$) with values near $0 m s^{-1}$ shaded cyan, c) spectrum width ($m s^{-1}$), d) the total power (P_{tot}) field, e) the clutter power (C_p) field and f) the power near zero (P_{nz}) field. Notice the good discrimination between NP clutter and precipitation return.

discriminating between convective precipitation return and clutter return. Clutter typically has a narrow spectrum while convective precipitation has a broad spectrum. Stratiform precipitation is not being considered in this discussion. When Ratio 1 is large then the majority of the power is at the velocity index g_0 and may be a good indicator of clutter return. Likewise, when Ratio 2 is large, this indicates that the majority of the power is at the g_0 velocity index rather than in the P_{nz} region and suggests a narrow spectrum at g_0 . Clutter return may be indicated when both ratios are large.

To illustrate these new variables, both ratios are calculated using time series data from the Norman WSR-88D (KOUN) radar. The variables P_{tot} , C_p and P_{nz} are shown in Figure 7 with the moment data. As suggested in the above discussion, these variables show a good ability to discriminate between precipitation and clutter return for this

example. The results of calculating Ratio 1 and Ratio 2 are shown in Figure 8. These results show that both Ratios tend to be large within clutter when compared to the precipitation return.

Before these new variables can be input into the REC APDA or PDA, membership functions must be devised. Additional cases will need to be examined to ascertain the generality of the results. Further, because stratiform precipitation also can have a narrow spectrum width and appear much like clutter return in the spectral domain, these Ratios must be examined within stratiform precipitation return.

As a first example, these new spectral domain variables show considerable promise for the REC and may lead to improved performance in certain situations.

8. Summary

An update on the AP Clutter Mitigation Scheme for the WSR-88D has been given. Recent results from the REC and the Z-Comp algorithms were shown for a Denver snow case. A comparison was made between surface measurements of snowfall accumulation and radar-derived snowfall accumulation. New spectral domain variables were presented that will be input into the REC in preparation for future implementation within the ORDA.

9. Acknowledgements

The NOAA Radar Operations Center (ROC), Norman, OK, and the United Arab Emirates (UAE) sponsored this research. The National Severe Storms Laboratory (NSSL) is thanked for providing the KOUN time series data.

10. References

Ellis, S.M., 2001: Compensating reflectivity for clutter filter bias in the WSR-88D, *Preprints, 17th Int'l IIPS Conf.*, AMS, Albuquerque, NM, 14-18 Jan 2001, 142-145.

Ellis, S., C. Kessinger, T.D. O'Bannon, and J. Van Anandel, 2003: Mitigating ground clutter contamination in the WSR-88D. *Preprints-CD, 19th Int'l IIPS Conf.*, AMS, Long Beach, 9-13 Feb 2003.

Elvander, R.C., S.M Holt, B. Bumgarner and R. Ice, 2001: Weather surveillance radar – 1988 Doppler (WSR-88D) open radar data acquisition (ORDA) enhancements. *Preprints, 30th International Conference on Radar Meteorology*, American Meteorological Society, Munich, Germany, 19-24 July 2001, p. 694-697.

Fulton, R.A., J.P. Breidenback, D.J. Seo, D.A. Miller, and T. O'Bannon, 1998: The WSR-88D rainfall algorithm. *Weather and Forecasting*, **13**, 377-395.

Keeler, R.J., J. Lutz and J. Vivekanandan, 2000: S-Pol: NCAR's polarimetric Doppler research radar, *IGARRS-2000, IEEE*, Honolulu, HI, 24-28 Jul 2000, 4pp.

Keeler, R., J. Hubbert, and J. Lutz, 2003: NEXRAD data quality by spectral processing, Spectral processing on NCAR's S-Pol radar. *Preprints, IGARSS-2003*, Toulouse, France, 21-25 July 2003.

Kessinger, C., S. Ellis, and J. Van Anandel, 1999: A fuzzy logic, radar echo classification scheme for the WSR-88D. *Preprints, 29th International Radar Meteorology Conference*, American Meteorology Society, 12-16 July 1999, Montreal, Canada, 576-579.

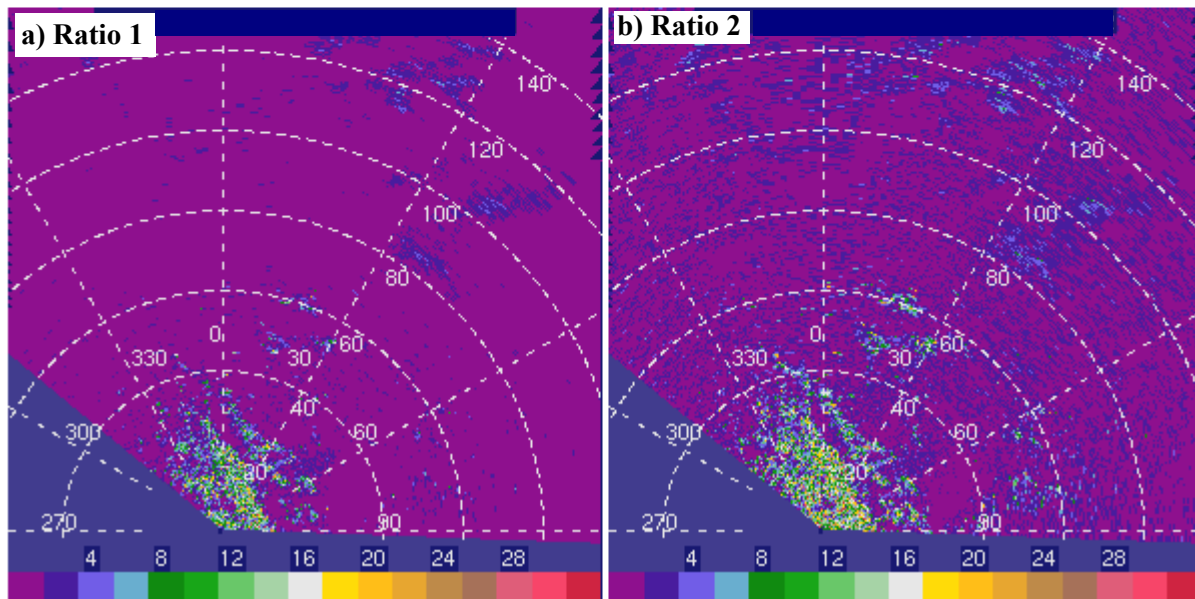


Figure 8. The results of the Ratio 1 and Ratio 2 calculations are shown for the KOUN data shown in Figure 7.

- Kessinger, C., S. Ellis, and J. Van Andel, 2002: NEXRAD Data Quality: An update on the AP clutter mitigation scheme. *Preprints, 18th International Conference on Interactive Information and Processing Systems (IIPS) for Meteorology, Oceanography, and Hydrology*, American Meteorological Society, Orlando, 13-17 January 2002, p. 127-129.
- Kessinger, C., S. Ellis and J. Van Andel, 2003: The radar echo classifier: a fuzzy logic algorithm for the WSR-88D. *Preprints-CD, 3rd Conf. Artificial Applications to Environmental Science*, AMS, Long Beach, 9-13 Feb 2003.
- Kosko, B., 1992: *Neural Networks and Fuzzy Systems: A Dynamical Systems Approach to Machine Intelligence*. Prentice-Hall, N.J.
- O'Bannon, T., 1998: The enhanced WSR-88D precipitation processing subsystem. *Preprints, 14th International Conference on Interactive Information and Processing Systems (IIPS) for Meteorology, Oceanography, and Hydrology*, American Meteorological Society, Phoenix, AZ, 11-16 Jan. 1998, 267-270.
- O'Bannon, T., and F. Ding, 2003: Continuing enhancement of the WSR-88D precipitation processing subsystem. *Preprints, 31st Int'l Conf. on Radar Meteorology*, AMS, 6-12 August 2003.
- Saffle, R.E., M.J. Istok and L.D. Johnson, 2001: NEXRAD open systems – progress and plans. *Preprints, 30th International Conference on Radar Meteorology*, American Meteorological Society, Munich, Germany, 19-24 July 2001, p. 690-693.
- Smith, P.L., 1984: Equivalent radar reflectivity factors for snow and ice particles, *Journal of Climate and Applied Meteorology*, **23**, 1258-1260.
- Steiner, M., R.A. Houze, Jr., S.E. Yuter, 1995: Climatological characterization of three-dimensional storm structure from operational radar and rain gauge data. *Journal of Applied Meteorology*, **34**, 1978-2007.
- Super, A.B., and E.W. Holroyd, 1997: Snow accumulation algorithm development for the WSR-88D radar. *Preprints, 28th Conf. Radar Meteorology*, AMS, Austin, 7-12 September 1997, 324-325.

